Eur. Phys. J. C 11, 301–307 (1999)
Digital Object Identifier (DOI) 10.1007/s100529900184

THE EUROPEAN PHYSICAL JOURNAL C

Probing a nucleon spin structure at TESLA by the real polarized gamma beam

S. Alekhin[1], V. Borodulin[1], A. Çelikel[2], M. Kantar[2], S. Sultansoy[2,3]

[1] IHEP, Protvino, Russia
[2] Ankara University, Ankara, Turkey
[3] Institute of Physics, Baku, Azerbaijan

Received: 22 March 1999 / Revised version: 17 June 1999 / Published online: 14 October 1999

Abstract. The recent proposals concerning the usage of the real polarized gamma beam, obtained by Compton backscattering of the laser photons off the electron beams from either the linear or circular accelerators were considered. The heavy quark photoproduction process, which gives a unique opportunity to measure the polarized gluon distribution, was investigated.

1 Introduction

A spin crisis arose when the first determination of

$$\Delta\Sigma = \Delta u + \Delta d + \Delta s$$

was found to be much smaller than expected [1], where

$$\Delta f \equiv \int \mathrm{d}x \Delta f(x, Q^2),$$

and the $f(x, Q^2)$ are the polarized quark spin distribution functions. The recent value of the world average for $\Delta\Sigma$ is approximately 0.3 ± 0.06. This is much smaller than the relativistic quark model prediction of 0.6 [2]. Among the various explanations of the EMC results on the longitudinally polarized proton structure function, that of the perturbative QCD approach occupies a prominent position and opens a new domain of tests [3]. It has been shown that in perturbative QCD, predictions of the quark-parton model concerning the singlet axial charge contribution to I_1^p need to be modified because of the γ_5 anomaly of the flavor singlet current J_μ^5. In this approach, the main question is the magnitude of the polarized gluon distribution. But there is a great uncertainty in theoretical estimates of the magnitude and x-dependence of $\Delta G(x)$, especially in the moderate x-region $x > 0.1$. One calculation, performed in the framework of MIT bag model, predicts a negative $\Delta G(x)$ value, thus even sharpening the problem [4].

In order to measure the gluon contribution to the nucleon spin, we must select a process where the familiar lowest order graphs of deep inelastic scattering from a single quark are suppressed. Analysis of the experimental data shows that there is no significant charm content in the nucleons [5]. Then one may hope to be able to determine polarized gluon effects in the process of the charmed quark photoproduction. Due to the comparatively large mass of the c-quark the leading mechanism for obtaining a $c\bar{c}$-pair in the final state is the hard photon–gluon fusion (PGF) process

$$\gamma + g \to c + \bar{c} \tag{1}$$

and the $c\bar{c}$-pair produced may form a J/ψ meson, or fragment separately into open charm states.

A rich spin physics program was proposed by the COMPASS collaboration at CERN [6]. A large part of it is devoted to the measurement of gluon polarization by tagging D^0, D^{*+}-mesons produced in the $\gamma^* N$ collisions. The produced D^0, D^{*+}-mesons will be reconstructed from their two-and three-body decays into hadrons. It permits one to impose constraints on the invariant masses of $K\pi\pi$, $K\pi, \cdots$ subsystems, which effectively reject a background, especially in the case of D^{*+}-tagging. The statistical precision on the polarization asymmetry measurement is expected to be about 0.05.

A proposal has been made [7] to determine $\Delta G(x)$ from the measurement of the asymmetry in the charm photoproduction process in the scattering of polarized real photons off a polarized fixed target. In this paper we consider the possibility to realize this experiment at the TESLA machine [8], and discuss briefly an opportunity to perform it at SLAC and LEP2.

2 The real gamma beam

2.1 Linear accelerator

The scheme of the proposed experiment looks like as follows. A circularly polarized laser beam with a photon energy $\omega_0 = 3.3\,\mathrm{eV}$ (Cu15 laser) is scattered off the 250(50)

GeV-electrons provided by TESLA (SLAC) [9]. Throughout this subsection the numbers in parentheses refer to the SLAC gamma beam parameters. The Compton backscattered photon beam has a spectrum $\gamma(y)$, with

$$\gamma(y) = \frac{1}{N} \times \frac{\mathrm{d}N}{\mathrm{d}y}, N = \int \mathrm{d}y \frac{\mathrm{d}N}{\mathrm{d}y},$$
$$\frac{\mathrm{d}N}{\mathrm{d}y} = \frac{1}{1-y} + 1 - y - 4r(1-r), \qquad (2)$$

and closely follows the trajectory of the primary electron beam. Here the ratio of the hard photon energy ω to the electron energy E_e has a range

$$y = \frac{\omega}{E_e}, \quad 0 \le y \le y_{max} = \frac{\kappa}{1+\kappa} \sim 0.927(0.717),$$
$$\kappa = \frac{4\omega_0 E_e}{m_e^2} \sim 12.638(2.528), \quad r = \frac{y}{\kappa(1-y)}. \qquad (3)$$

Had the laser beam been circularly polarized, the γ-beam would have been polarized too and the γ-beam helicity would have been given by

$$\xi_2 = \frac{B(y)}{N\gamma(y)},$$
$$B(y) = -\lambda_{\mathrm{ph}}(2r-1)\Big(\frac{1}{1-y} + 1 - y\Big), \qquad (4)$$

where λ_{ph} denotes the laser photon helicity. The Compton spectrum (2) and the γ-beam polarization (4) refer to the scattering of the polarized laser light off the unpolarized electron beam both for the linear and circular accelerators. But the SLAC and TESLA electron beams are polarized, so the usage of (2) and (4) in this case implies that one deals with the average over different electron beam polarizations.

Due to the unique dependence of both the γ-beam energy and the polarization on the scattering angle θ_γ between the incident and scattered photon,

$$\theta_\gamma(\omega) \sim \frac{m_e}{E_e}\sqrt{\frac{E_e\kappa}{\omega} - (\kappa+1)},$$

it is possible to obtain an almost monochromatic gamma beam with energy $0.99\omega_{max} \le \omega \le \omega_{max}$ and polarization nearly equal to unity by selecting photons with $\theta_\gamma \le 0.759(1.93) \cdot 10^{-6}$ rad. Taking the distance between the conversion region and the collimator to be 100 m, we obtain that this angle corresponds to the diameter of the selecting slit, $d = 152(386)\,\mu$m.

In our further estimation on the luminosity of the gamma beam scattering off a polarized fixed target, we shall follow the method outlined in [10]. We determine the optimal number of converted photons N_γ by the required to obtain one event per collision,

$$\beta N_\gamma T_n \sigma_{\gamma p} = 1, \qquad (5)$$

where β is the fraction of the photons coming through the slit, T_n stands for the target nucleon density and $\sigma_{\gamma p}$ is the total cross section of the gamma–proton collisions. In the case of 1% γ -beam monochromaticity $\beta \sim 4.22(2.02) \cdot 10^{-2}$, for a deuterated butanol target with a length of about 40 cm the density is $T_n = 4 \cdot 10^{25}\,\mathrm{cm}^{-2}$ and $\sigma_{\gamma p} \sim 100\,\mu$b at high energies, so we get $N_\gamma = 5.92(12.36) \cdot 10^3$. Because the number of electrons in a bunch is $N_e = 5.15(3.5) \cdot 10^{10}$ for TESLA (SLAC), we obtain the necessary conversion coefficient

$$K = \frac{N_\gamma}{N_e} = 1.15(3.53) \cdot 10^{-7}.$$

The number of photons required to provide the scattering of each electron with the laser photon is defined by

$$\frac{n_0\sigma_c}{S_{\mathrm{eff}}} = 1, \qquad (6)$$

where n_0 is the number of photons in a laser pulse, $\sigma_c = 1.1(2.59) \cdot 10^{-25}\,\mathrm{cm}^2$ is the total Compton cross section and S_{eff} is the effective area of the photon and electron beams intercept. Choosing $S_{\mathrm{eff}} = 4 \cdot 10^{-6}\,\mathrm{cm}^2$, one can easily get the laser energy per pulse,

$$A_0 = n_0\omega_0 \sim 19.2(8.152)\,\mathrm{J},$$

corresponding to the total electron conversion. Since the optimal number of converted photons N_γ, defined by (5), is much less than N_e, we do not need total conversion of the electrons and the required pulse energy is suppressed by the factor K:

$$A = KA_0 \sim 2.21(2.88) \cdot 10^{-6}\,\mathrm{J},$$

which is accessible with modern laser technology.

Finally, we shall discuss the choice of the laser pulse frequency. It should evidently coincide with the linac frequency f_{pulse} when the number of bunches n_{b} in the electron beam is equal to unity. If the electron beam has a multibunch structure, one may either choose the repetition rate of the laser pulses to be equal to $f_{\mathrm{pulse}} \cdot n_{\mathrm{b}}$ or use a mirror system [11], which evidently decreases the laser pulse frequency. Since a detailed discussion of the experimental setup is beyond the scope of our paper, we for simplicity choose the laser pulse frequency to be equal to $f_{\mathrm{pulse}} \cdot n_{\mathrm{b}}$.

For the linear accelerators the integrated luminosity per year of operation takes the form

$$L^{\mathrm{int}}_{\mathrm{linac}} = 10^7 \cdot f_{\mathrm{rep}}\beta N_e K T_n, \qquad (7)$$
$$f_{\mathrm{rep}} = f_{\mathrm{pulse}} \cdot n_{\mathrm{b}},$$

where f_{rep} is the collision frequency. Taking into account (5), one can estimate $L^{\mathrm{int}}_{\mathrm{linac}}$ as follows:

$$L^{\mathrm{int}}_{\mathrm{linac}} = 10^7 \cdot \frac{f_{\mathrm{rep}}}{\sigma_{\gamma p}} \sim 0.8(0.012)\,\mathrm{fb}^{-1}. \qquad (8)$$

Table 1. The parameters of the LEP2, SLAC and TESLA electron beams. Here $f_{\rm pulse}$ is the pulse frequency, H and V are the horizontal and vertical beam radius respectively, N_e is the number of electrons per bunch and $n_{\rm b}$ is the number of bunches

	E_e (GeV)	$N_e(10^{10})$	$n_{\rm b}$	$f_{\rm pulse}$ (Hz)	H (μm)	V (μm)
LEP2	100	40	4	$11.25 \cdot 10^3$	200	8
SLAC	50	3.5	1	120	2.1	0.6
TESLA	250	5.15	800	10	0.64	0.1

Table 2. The real gamma beam parameters at LEP2, SLAC and TESLA. Here $y_{\max}$ is the ratio of the maximal gamma beam energy to the electron energy, θ_γ is the opening angle of the collimator, β denotes the fraction of photons coming through the slit, N_γ is the total number of converted photons, K is the conversion coefficient and A is the laser energy per pulse

	$y_{\max}$	θ_γ (10^{-6} rad)	β	N_γ (10^4)	K (10^{-7})	A (10^{-6} J)	$L^{\rm int}$ (fb^{-1})
LEP2	0.835	1.26	0.0265	0.945	0.236	13.4	0.27
SLAC	0.717	1.93	0.0202	1.236	3.53	2.88	0.012
TESLA	0.927	0.759	0.0422	0.592	1.15	2.21	0.8

2.2 Circular accelerator

Now we briefly consider the possibility to obtain the real gamma beam at a circular electron accelerator, say at LEP2. All calculations are done in analogy with the TESLA case, except for a few details. First of all, $f_{\rm rep}$ now takes the form

$$f_{\rm rep} = f_{\rm pulse} \cdot n_{\rm b} = \frac{c}{2\pi R} \cdot n_{\rm b} = 44980\,{\rm Hz},$$

where the number of electron bunches $n_{\rm b} = 4$, c is the speed of light, R is the ring radius and $f_{\rm pulse}$ is the circulation frequency in this case. It is evident that for the circular accelerator $f_{\rm rep}$ should coincide with the frequency of the laser pulses. The next remark concerns (6). We choose the effective area of the photon and electron beams intercept to be $S_{\rm eff} \sim S_e = 2 \cdot 10^{-4}\,{\rm cm}^2$, where S_e is the transverse area of the LEP2 electron beam, and the total Compton cross section $\sigma_c = 1.86 \cdot 10^{-25}\,{\rm cm}^2$ at the LEP2 energy. And finally, we should take into account the effects of beam mean life time (we did not consider these effects before, since every electron bunch provided by the linear accelerator could be used only once).

In each collision, about KN_e electrons are scattered. Since every bunch collides with the frequency $f_{\rm pulse} = c/2\pi R \sim 1.12 \cdot 10^4\,{\rm Hz}$, the mean lifetime of the beam $\tau_{\rm b}$ may be estimated to be

$$\tau_{\rm b} = \frac{\log(1-\delta)}{\log(1-K)} \cdot \frac{1}{f_{\rm pulse}} \sim 400\,{\rm s},$$

where δ denotes the maximal fraction of the electron loss permitted by the beam dynamics. In what follows we choose $\delta = 0.1$; then the number of collisions each bunch makes during one cycle is equal to

$$l = \frac{\log(1-\delta)}{\log(1-K)} \sim 4.46 \cdot 10^6,$$

and the mean number of electrons in a bunch $\hat{N}_e$ is given by

$$\hat{N}_e = (1 - \frac{l}{2}k)N_e,$$

where N_e denotes the initial number of electrons in a bunch.

For the ring accelerators the integrated luminosity per year of operation takes the form

$$L^{\rm int}_{\rm ring} = 10^7 \cdot \frac{\tau_{\rm b}}{\tau_{\rm a} + \tau_{\rm b} + \tau_{\rm f}} f_{\rm rep} \beta \hat{N}_e K T_n, \qquad (9)$$

where $\tau_{\rm a}$ is the acceleration time, and $\tau_{\rm f}$ is the filling time. Taking into account (5), one can estimate $L^{\rm int}_{\rm ring}$ as follows:

$$L^{\rm int}_{\rm ring} = 10^7 \cdot \frac{\tau_{\rm b}}{\tau_{\rm a} + \tau_{\rm b} + \tau_{\rm f}} f_{\rm rep} \frac{\hat{N}_e}{N_e} \frac{1}{\sigma_{\gamma p}} \sim 0.27\,{\rm fb}^{-1}. \qquad (10)$$

The electron beam parameters we have used in the estimations can be seen in Table 1, while the γ-beam characteristics are given in Table 2.

Thus the luminosity at a probable SLAC experiment is about one order of magnitude smaller compared with the LEP2 case due to a lower collision frequency. Choosing a more powerful laser one can reach almost the same luminosity at SLAC, but the price will be too high: more than one hundred events per collision, which significantly reduces the range of physical phenomena accessible for investigations. The luminosity at TESLA even exceeds that of the LEP2, since the TESLA project will operate with multibunch trains.

3 The heavy quark photoproduction

The differential cross section of the photon–gluon fusion looks like as follows:
[12]

$$\frac{{\rm d}\hat{\sigma}}{{\rm d}\hat{t}} = \frac{{\rm d}\hat{\sigma}^n}{{\rm d}\hat{t}} + \lambda_g \xi_2 \frac{{\rm d}\delta\hat{\sigma}}{{\rm d}\hat{t}},$$

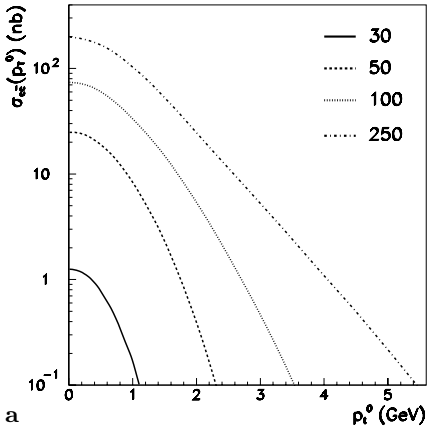

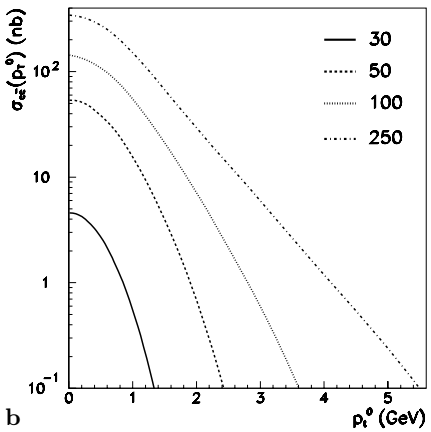

Fig. 1a,b. The distribution of charm production $\sigma_{c\bar{c}}(p_\mathrm{t} \geq p_\mathrm{t}^0)$ versus p_t^0 for different electron energies: $E_e = 30\,\mathrm{GeV}$, solid line, $E_e = 50\,\mathrm{GeV}$, dashed line, $E_e = 100\,\mathrm{GeV}$, dotted curve, $E_e = 250\,\mathrm{GeV}$, dashed-dotted line. The c-quark mass is $m_c = 1.5\,\mathrm{GeV}/c^2$ **a**, $m_c = 1.3\,\mathrm{GeV}/c^2$ **b**

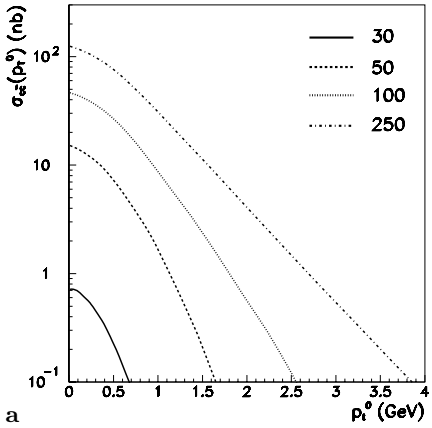

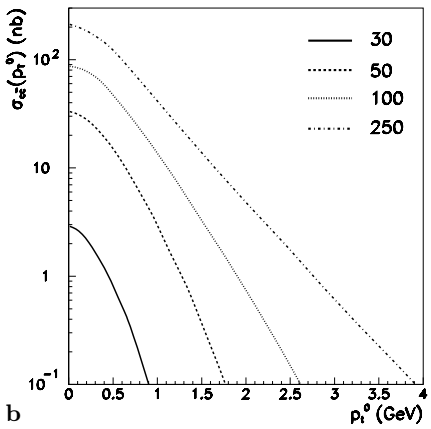

Fig. 2a,b. The distribution of the inclusive D^*-meson production $\sigma_{D^*X}(p_\mathrm{t} \geq p_\mathrm{t}^0)$ versus p_t^0 for different electron energies: $E_e = 30\,\mathrm{GeV}$, solid line, $E_e = 50\,\mathrm{GeV}$, dashed line, $E_e = 100\,\mathrm{GeV}$, dotted curve, $E_e = 250\,\mathrm{GeV}$, dashed-dotted line. The c-quark mass is $m_c = 1.5\,\mathrm{GeV}/c^2$ **a**, $m_c = 1.3\,\mathrm{GeV}/c^2$ **b**

where λ_g and ξ_2 denote the gluon and photon helicities. The spin averaged and polarized asymmetry distributions in the LO QCD take the form, respectively, of

$$\frac{\mathrm{d}\hat{\sigma}^n}{\mathrm{d}\hat{t}} = \frac{\pi\alpha\alpha_s(s)e_q^2}{\hat{s}^2}\left(\frac{4m^2\hat{s}}{(\hat{t}-m^2)(\hat{u}-m^2)} + \frac{\hat{u}-m^2}{\hat{t}-m^2} + \frac{\hat{t}-m^2}{\hat{u}-m^2} - \frac{4m^4\hat{s}^2}{(\hat{t}-m^2)^2(\hat{u}-m^2)^2}\right). \quad (11)$$

$$\frac{\mathrm{d}\delta\hat{\sigma}}{\mathrm{d}\hat{t}} = \frac{\pi\alpha\alpha_s(s)e_q^2}{2\hat{s}^2}\left(\left(\frac{\hat{u}-m^2}{\hat{t}-m^2} + \frac{\hat{t}-m^2}{\hat{u}-m^2}\right)^2 - \hat{s}(\hat{s}-4m^2)\left(\frac{1}{(\hat{t}-m^2)^2} + + \frac{1}{(\hat{u}-m^2)^2}\right)\right), \quad (12)$$

Here $\hat{s}, \hat{t}, \hat{u}$ are the invariant variables of the subprocess, $\alpha, \alpha_\mathrm{s}(s)$ are the fine and strong coupling constants respectively and e_q denotes the c-quark charge.

The produced $c\bar{c}$ pairs can form J/ψ or fragment into D, D^*-mesons. In what follows we shall consider only the open charm production, because this process is more transparent from a theoretical point of view. In addition, the open charm has an advantage over J/ψ production, because its cross section is at least ten times larger for the attainable photon energies.

The accumulated p_t-distribution of the charmed quarks

$$\sigma_{c\bar{c}}(p_\mathrm{t}^0) = \int\limits_{p_\mathrm{t} \geq p_\mathrm{t}^0} \mathrm{d}p_\mathrm{t} \int \frac{\mathrm{d}\hat{s}}{s}\frac{\mathrm{d}\hat{\sigma}^n}{\mathrm{d}p_\mathrm{t}} G(x, Q^2) \quad (13)$$

versus p_t^0 is shown in Fig. 1, and Fig. 2 presents the same dependence for the inclusive D^*-meson production

$$\sigma_{D^*}(p_\mathrm{t}^0) = \sigma_{D^{*+}}(p_\mathrm{t}^0) + \sigma_{D^{*0}}(p_\mathrm{t}^0).$$

In our estimates we have used the parametrizations of both polarized and unpolarized gluon densities from [13], c-quark fragmentation functions were taken from [14], α_s from the global analysis of the DIS data [15]. The gamma beam spectrum was chosen monochromatic with energy $E_\gamma = \kappa/(1+\kappa)E_e$ for $E_e \geq 50\,\mathrm{GeV}$, while for $E_e = 30\,\mathrm{GeV}$ the smeared-out spectrum, given by (2), was used. Numerical integration was performed with the

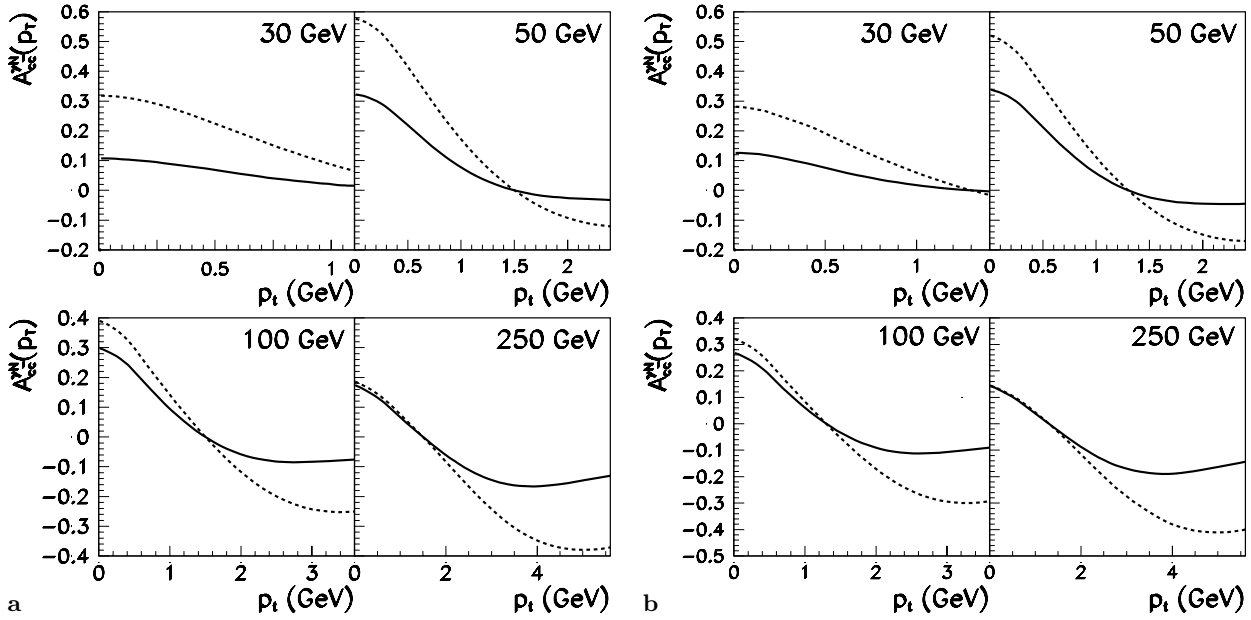

Fig. 3a,b. The differential asymmetry $A_{c\bar{c}}^{\gamma N}(p_{\rm t})$ of the c-quark production versus $p_{\rm t}$ for the c-quark mass equal to $1.5\,{\rm GeV}/c^2$ **a**, $1.3\,{\rm GeV}/c^2$ **b**. The solid (dashed) line corresponds to the set A (B) of the polarized gluon density [13]

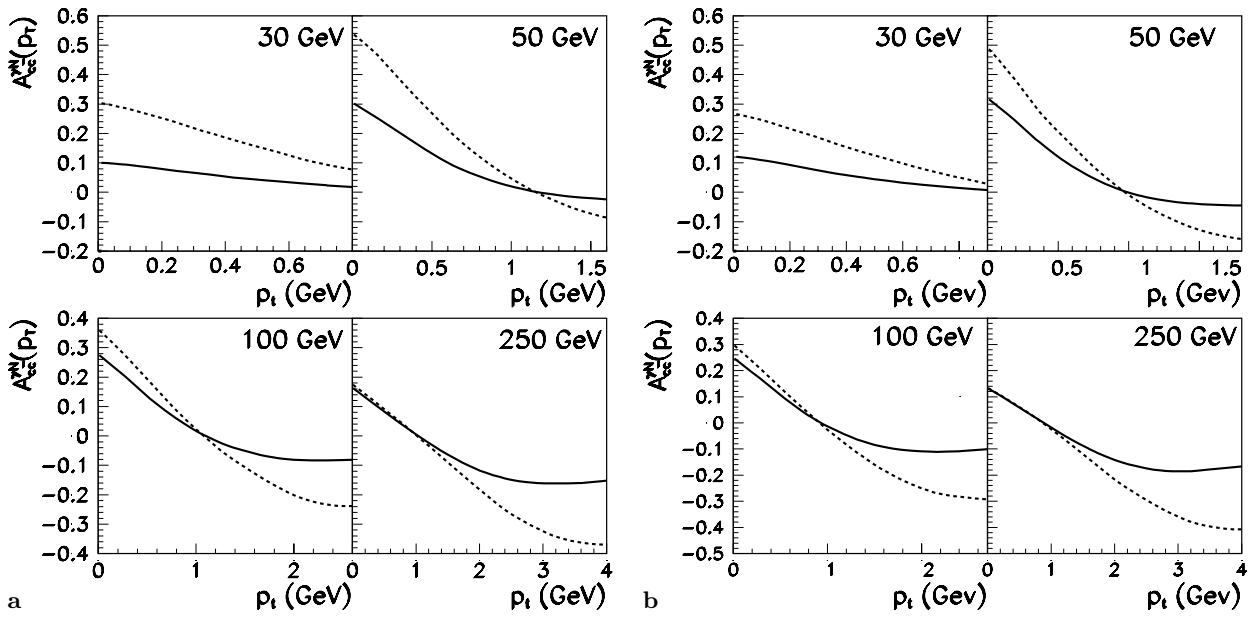

Fig. 4a,b. The differential asymmetry $A_{D^*}^{\gamma N}(p_{\rm t})$ of the D^* meson production versus $p_{\rm t}$ for the c-quark mass equal to $1.5\,{\rm GeV}/c^2$ **a**, $1.3\,{\rm GeV}/c^2$ **b**. The solid (dashed) line corresponds to the set A (B) of the polarized gluon density [13]

help of the adaptive integration code of [16]. All distributions have a similar form and decrease exponentially with increasing $p_{\rm t}^0$ when the transverse momentum exceeds $1\,{\rm GeV}/c$. One concludes that the estimated production rate of D^*-mesons with large transverse momentum $p_{\rm t} \geq 1\,{\rm GeV}/c$ is sizeable and reaches approximately 30 nb (40 nb) at TESLA energy for a c-quark mass equal to $1.5(1.3)\,{\rm GeV}/c^2$, respectively.

The differential asymmetry $A_{c\bar{c}}^{\gamma N}(p_{\rm t})$ of the c-quark production versus $p_{\rm t}$,

$$A_{c\bar{c}}^{\gamma N}(p_{\rm t}) = \frac{{\rm d}\delta\sigma}{{\rm d}p_{\rm t}} \Big/ \frac{{\rm d}\sigma^n}{{\rm d}p_{\rm t}}, \tag{14}$$

is shown in Fig. 3 for a c-quark mass of $1.5(1.3)\,{\rm GeV}/c^2$, and the analogous dependences for D^*-meson production are pictured in Fig. 4 for the same mass set. Here we have introduced the following notations:

$$\frac{{\rm d}\sigma^n}{{\rm d}p_{\rm t}} = \int \frac{{\rm d}\hat{s}}{s} \frac{{\rm d}\hat{\sigma}^n}{{\rm d}p_{\rm t}} G(x, Q^2),$$
$$\frac{{\rm d}\delta\sigma}{{\rm d}p_{\rm t}} = \int \frac{{\rm d}\hat{s}}{s} \frac{{\rm d}\delta\hat{\sigma}}{{\rm d}p_{\rm t}} \Delta G(x, Q^2).$$

As is already known, the differential asymmetry of $c\bar{c}$ production, derived in the leading order (LO) approximation, has a kinematic zero at $p_{\rm t} = m_c$ and then changes sign. For D^*-meson production the zero position shifts to the lower value of $p_{\rm t} \sim 1\,{\rm GeV}/c$ due to fragmentation smearing. Integration over the total range of $p_{\rm t}$ evidently decreases the asymmetry, so it is reasonable to introduce a kinematic cut on the D^*-meson transverse momentum, say $p_{\rm t} \geq 1\,{\rm GeV}/c$. In this region $A^{\gamma N}_{D^*}(p_{\rm t})$ does not change sign; moreover, the predicted asymmetry value heavily depends on the choice of the polarized gluon distribution. This is due to the fact that the main contribution to the production of the D^*-mesons having a large transverse momentum comes from the region $x \geq 0.1$, where $\Delta G(x, Q^2)$ is poorly known. At present, there are plausible restrictions on the polarized gluon density only at $x \leq 0.1$, where all model predictions almost coincide. Then the precise measurement of the polarized gluon density at $x \geq 0.1$ will surely help to choose a reasonable parametrization of $\Delta G(x, Q^2)$.

We remind the reader that our estimates were performed only in the LO approximation. The next-to-leading order (NLO) corrections, recently derived in [17], turned out quite sizeable, which underscores once more the necessity of the NLO results. But the shape of the NLO distributions is similar to the LO one and this partially simplifies the problem of taking account of the NLO corrections. We shall not discuss this topic in detail since it is beyond the scope of our paper.

4 Event reconstruction

4.1 D^*-tagging

One of the best methods for D^*-tagging uses the kinematic constraint of the decay chain:

$$D^* \to D\pi \to (K\pi)\pi. \tag{15}$$

The difference of the invariant masses,

$$\begin{aligned} \Delta M &= m(K\pi\pi) - m(K\pi) = \\ &= m(D^*) - m(D) \sim 145\,{\rm MeV}/c^2, \end{aligned} \tag{16}$$

is very close to the π-meson mass, and can be determined with a precision of about $2.5\,{\rm MeV}/c^2$ [6], significantly exceeding the accuracy of the D^*-meson mass measurement. This permits one to substantially reduce the background to the D^{*+}-meson production; for example, COMPASS estimates showed that the background is less than 10%.

The isospin invariance suggests equal D^{*+} and D^{*0} production rates; then $\sigma(D^{*+}X) \sim 0.5 \cdot \sigma(D^*X)$. Since the branching ratio for the decay chain (15) is 2.6%, about $\sim 62.4 \cdot 10^4$ $(83.2 \cdot 10^4)$ D^{*+}-mesons with $p_{\rm t}$ exceeding $1\,{\rm GeV}/c$ will be produced at TESLA energy in a year. Assuming the overall acceptance to be equal to 0.2 [6], we expect to reach a reconstruction rate of

$$N_{D^{*+}} = 124.8 \cdot 10^3 (166.4 \cdot 10^3) \cdot {\rm year}^{-1}. \tag{17}$$

Table 3. The target parameters. Here $P_{\rm t}$ is the target polarization, $f_{\rm t}$ denotes the fraction of the polarized target nucleons, T_n stands for the target density, and L is the target length

	$f_{\rm t}$	$P_{\rm t}$	T_n $(10^{25}\,{\rm cm}^{-2})$	L (cm)
butanol	0.24	0.8	4	40

Table 4. The registration rates of D^{*+} mesons at TESLA. Here σ is the cross section of the inclusive D^* meson production, $N_{D^{*+}}$ denotes the total number of observed D^{*+} mesons per year taking account of the efficiency, and $\Delta A^{\gamma N}_{D^{*+}}$ stands for the statistical precision

	$\sigma(nb)$	$N_{D^{*+}}$ (10^3)	$\Delta A^{\gamma N}_{D^{*+}}$ (10^{-2})
$p_{\rm t} \geq 0$	126 (215)	524.2 (894.4)	0.72 (0.55)
$p_{\rm t} \geq 1\,{\rm GeV}/c$	30 (40)	124.8 (166.4)	1.47 (1.28)
$p_{\rm t} \geq 2\,{\rm GeV}/c$	4.1 (5)	17.1 (20.8)	3.99 (3.61)

A rigorous evaluation of the acceptance will change these figures, because the COMPASS experiment uses kinematic cuts different from ours. Nevertheless, the equality (17) gives a good idea of the actual reconstruction rate attainable in the proposed experiment.

The observed spin asymmetry $A^{\rm exp}_{D^*}$ of the D^{*+}-meson photoproduction taking account of the beam and target polarizations is given by

$$A^{\rm exp}_{D^*} = P_{\rm b} P_{\rm t} f_{\rm t} A^{\gamma N}_{D^*}. \tag{18}$$

Here the asymmetry $A^{\gamma N}_{D^*}$ is the ratio of the helicity dependent and the helicity averaged cross sections for D^{*+}-meson production in γN-collisions, calculated taking into account the kinematic cuts. The parameters $P_{\rm b}$ and $P_{\rm t}$ are the beam and target polarizations, and $f_{\rm t}$ denotes the fraction of the polarized target nucleons. The target characteristics are given in Table 3, while the gamma beam polarization $P_{\rm b}$ is about unity.

We impose a $p_{\rm t}$ cut on the D^*-meson transverse momentum and choose three values of $p_{\rm t}$: 0, 1 and $2\,{\rm GeV}/c$. The statistical precision of $A^{\gamma N}_{D^*}$ taking into account the target properties is given by

$$\Delta A^{\gamma N}_{D^{*+}} \sim \frac{1}{\sqrt{N_{D^{*+}} f_{\rm t} P_{\rm b} P_{\rm t}}} = 2.08(1.81) \cdot 10^{-2}, \tag{19}$$

for the cut $p_{\rm t} \geq 1\,{\rm GeV}/c$. One can achieve an even better statistical precision by detecting D^* mesons in the total kinematic region of $p_{\rm t}$ (Table 4). On the other hand, a "strong" cut on the transverse momentum, say $p_{\rm t} \geq 2\,{\rm GeV}/c$, will lower the statistical accuracy by a factor of three, because the corresponding cross section does not exceed 3–4 nb. Our opinion is that the "moderate" restriction $p_{\rm t} \geq 1\,{\rm GeV}/c$ is best suited for the investigation of the gluon polarization. Under this cut the total cross section is still sizeable, which results in a reasonable value of the statistical precision; moreover, it permits one to decrease the background and reduce the uncertainties in the c-quark fragmentation process.

4.2 D^0 tagging

Experimentally, the total number of D^0-mesons per charm event is approximately equal to the sum of the D^{*+}- and D^{*0}-meson production rates. The produced D^0 may be detected via the simplest two-body decay,

$$D^0 \to K^- \pi^+,$$

with a branching ratio of 3.8%. An estimate shows that the D^0-meson reconstruction rate is more than the corresponding quantity for the D^{*+}-meson by a factor of three due to a larger value of both the D^0-production cross section and the decay branching ratio. However, unlike the D^{*+}-tagging, the background to the D^0-production remains significant even after taking into account the kinematic cuts, and it exceeds the signal, for example at COMPASS, by a factor of four [6]. This means that the correct evaluation of both the asymmetry and the statistical precision of the measurement requires a detailed analysis of the background, which is beyond the scope of our paper.

4.3 Single muon tagging

The most simple method to select charm production events consists in the detecting of muons from semileptonic D-meson decays. Muons coming from light meson decays, as well as Bethe–Heitler pairs, contribute mainly to the low values of $p_{\rm t}$, so one may reduce these backgrounds by imposing a cut on the D-meson transverse momentum, say $p_{\rm t} \geq 1\,{\rm GeV}/c$. Assuming the branching ratio of the decay

$$D^{0(+)} \to \mu + X,$$

to be 6.8% for the D^0 and 17.2% for the D^+-meson, and the ratio of the D-meson production rates per charm event to be

$$\frac{N_{D^0}}{N_{D^+}} \sim 3,$$

one may expect about $N_\mu = 4.51(6.02)\cdot 10^6$ prompt muons at TESLA for $m_c = 1.5, (1.3)\,{\rm GeV}/c^2$. On average, the muon acquires a transverse momentum equal to about one half of the parent meson mass, that is $1\,{\rm GeV}/c$ in our case. To obtain a rough estimate, suppose that only one half of the muons coming from decays of the D-mesons with $p_{\rm t} \geq 1\,{\rm GeV}/c$ will get a transverse momentum larger than $2\,{\rm GeV}/c$. In this case the reconstruction rate is given by

$$N_\mu \sim 2.26(3.01)\cdot 10^6,$$

under the assumption of 100% muon detection efficiency. The precision of the asymmetry measurement taking into account the target properties can be roughly estimated as

$$\Delta A_D^{\gamma N} \sim \frac{1}{\sqrt{N_\mu} f_{\rm t} P_{\rm b} P_{\rm t}} = 3.5(3.0)\cdot 10^{-3}. \qquad (20)$$

The exact evaluation of the statistical error requires a close investigation of the background. Nevertheless, (20) gives a good idea of the actual precision one may hope to reach at the TESLA experiment.

5 Conclusion

In the present paper we have considered the opportunity to use a polarized real photon beam for the investigation of the polarized gluon distributions. Our estimate corroborates the possibility to achieve a higher accuracy in the measurement of the charm photoproduction asymmetry compared with planned experiments at SLAC and CERN. The proposed experiment may give unambiguous information about both the total value and the x-dependence of the gluon polarization, which will permit one to significantly reduce the number of acceptable models decsribing the nucleon spin effects.

References

1. J. Ashman et al., Phys. Lett. B **206**, 364 (1988); J. Ashman et al., Nucl. Phys. B **328**, 1 (1989)
2. J. Ellis, R. Jaffe, Phys. Rev. D **9**, 1444 (1974); J. Eliis, R. Jaffe, Phys. Rev. D **10**, 1664 (1974) (E)
3. A. Efremov, O. Teryaev, JINR-E2-88-287 and Phys. Lett. B **240**, 200 (1990); G. Altarelli, G. Ross, Phys. Lett. B **212**, 391 (1988)
4. R.L. Jaffe, Phys. Lett. B **365**, 359 (1996)
5. J.J. Aubert et al., Phys. Lett. B **110**, 73 (1982)
6. COMPASS Proposal, CERN/SPSLC 96-14, SPSC/P 297
7. S. Alekhin, V. Borodulin, S. Sultansoy, Int. J. Mod. Phys. A **8**, 1603 (1993); S. Atag et al., Europhys. Lett. **29**, 815 (1995); Nucl. Instr. and Meth. A **381**, 23 (1996); M. Duren, in: Proceedings of the 2^{nd} Spin Workshop, Zeuthen, 1997, edited by J. Blumlein, A. DeRoeck, T. Gehrmann, W.D. Nowak (Springer, Berlin 1997), p. 414; V. Borodulin et al., the same Proceedings, p. 439
8. Conceptual design of a 500 GeV e^+e^- linear collider with integrated X-ray laser facility, edited by R. Brinkmann, G. Materlik, J. Rossbach, A. Wagner, DESY 1997-048, ECFA 1997-182
9. I.F. Ginzburg et al., Nucl. Instr. and Meth. **205**, 477 (1983)
10. S. Atag et al., Nucl. Instr. and Meth. A **381**, 21 (1996)
11. Ciftci et al., Nucl. Instr. and Meth. A **365**, 317 (1995)
12. G. Altarelli, W.J. Stirling, Particle World **1**, 40 (1989); W. Vogelsang, in: Physics at HERA, edited by W. Buchmuller, G. Ingelman (Springer, Berlin 1991), Vol. 1, p. 389
13. T. Gehrmann, W.J. Stirling, DTP/95/82, hep-ph/9512406
14. C. Peterson et al., Phys. Rev. D **27**, 105 (1983)
15. S.I. Alekhin, IHEP 96-79, hep-ph/9611293, 1996, to appear in Eur. Phys. J.
16. T.A. Merkulova, G.G. Takhtamyshev, JINR-E11-95-255, 1995
17. I. Bojak, M. Stratmann, DTP/98/22, hep-ph/9804353; I. Bojak, M. Stratmann, DTP/98/36, hep-ph/9807405